Medicinal Chemistry Research (2021) 30:473–482
https://doi.org/10.1007/s00044-020-02692-4

MEDICINAL CHEMISTRY RESEARCH

ORIGINAL RESEARCH

Structural insights of sulfonamide-based NLRP3 inflammasome inhibitors: design, synthesis, and biological characterization

Yiming Xu[1] · Matteo Scipioni[1] · Hallie Blevins[1] · Shijun Zhang[1]

Received: 16 November 2020 / Accepted: 8 December 2020 / Published online: 13 January 2021

Abstract

NLRP3 inflammasome has recently attracted much attention as a potentially druggable target to develop potential therapeutics for inflammatory and neurodegenerative disorders. In our continuing studies, structure–activity relationship studies were conducted based on a newly identified NLRP3 inhibitor, **YQ-II-128**, from our laboratory to understand the structural features and improve aqueous solubility. The results revealed that steric interactions at the propoxyl and amide domain of **YQ-II-128** are important for the observed inhibitory potency on the NLRP3 inflammasome. The results also identified the amide domain to incorporate polar moieties to improve solubility and potentially pharmacokinetic properties. As a result, analog **10** was identified as a selective NLRP3 inhibitor with comparable potency while significantly improved aqueous solubility. Collectively, these findings strongly encourage further optmization of **10** to develop analogs with improved pharmacokinetic properties as potential NLRP3-targted therapeutics.

Keywords NLRP3 inflammasome · SAR · Medicinal chemistry

Introduction

The innate immune system is at the forefront of immune responses in the detection of antigens and foreign invaders in the body [1]. These include pathogen associated molecular patterns (PAMPs) and damage associated molecular patterns (DAMPs), which are recognized through pattern recognition receptors (PRRs) [1, 2]. Amongst the characterized PRRs, the NOD-like receptors (NLRs), absent in melanoma 2 (AIM2)-like receptors, and retinoic acid-inducible gene I-like receptors recognize PAMPS and DAMPs in the cytosolic environment [2]. Architecturally, these cytosolic PRRs form a multiprotein complex called the inflammasome and consist of a sensor component, e.g., NLR, an adapter component (the apoptosis-associated speck-like protein containing a caspase-recruitment domain, ASC), and an effector component (pro-caspase-1) which is then converted into its active form, caspase-1, by proximity-induced cleavage [3]. Caspase-1 can then cleave other proteins into their active forms, including the pro-inflammatory cytokines of interleukin (IL)-1β and IL-18 [2–6]. Among the inflammasomes that have been identified and studied, the NLRP3 inflammasome is activated by plethora of stimuli and plays a significant role in the maturation and production of IL-1β and IL-18 [6]. The pathological roles of NLRP3 inflammasome dysregulation is evidenced by the gain-of-function mutations of NLRP3 in cryopyrin-associated periodic syndrome [7]. Recently, emerging evidence have linked the dysregulation of the NLRP3 inflammasome to a variety of human diseases, particularly those that are accompanied by the upregulation of inflammatory cytokines including inflammatory and neurodegenerative disorders [7–15]. Therefore, inhibiting the production and release of these inflammatory mediators would be of therapeutic value, highlighting the translational promise of this protein complex to develop effective NLRP3-targeted therapies for human diseases. This notion is further supported by the successful development of canakinumab, an IL-1β-neutralizing antibody; anakinra, a recombinant IL-1 receptor antagonist; and rilonacept, a decoy receptor that binds IL-1β and IL-1α [16–18].

Recently, small molecule inhibitors that directly inhibit the NLRP3 protein or indirectly interrupt the NLRP3 inflammasome signaling pathway have been reported [19]. This includes MCC950 [20], CY-09 [21], Oridonin [22],

✉ Shijun Zhang
szhang2@vcu.edu

[1] Department of Medicinal Chemistry, Virginia Commonwealth University, Richmond, VA 23298, USA

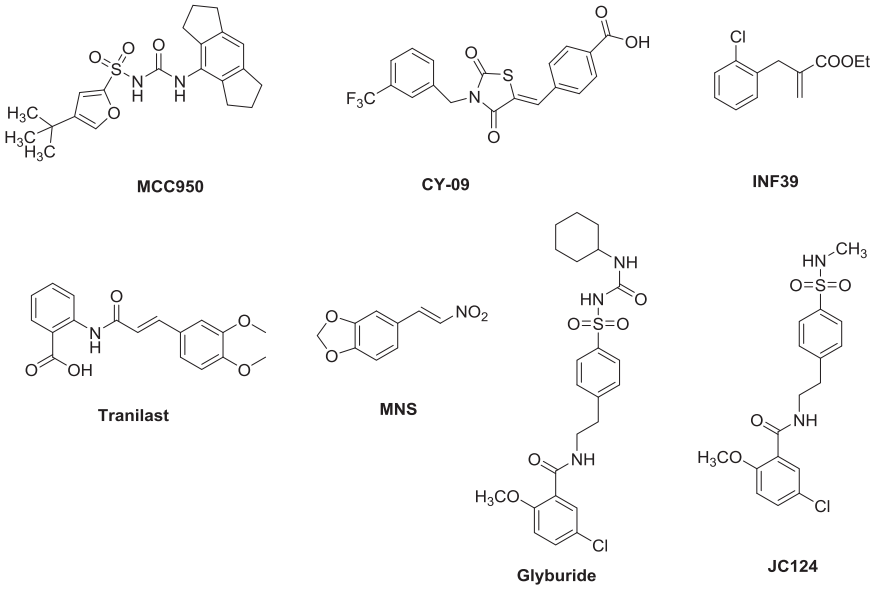

Fig. 1 Small molecule inhibitors of the NLRP3 inflammasome

Tranilast [23], MNS [24], OLT1177 [25], INF39 [26], and JC124 [27] (Fig. 1), among others. The demonstrated in vivo efficacy from various disease models by some of these inhibitors further supported the translational potential of targeting this protein complex [28–32]. Our laboratory has recently developed sulfonamide-based NLRP3 inhibitors and medicinal chemistry campaign led to a lead compound, **YQ-II-128**, that shows promising potency and selectivity to NLRP3 over other inflammasomes [27, 33] (Fig. 2). Furthermore, our ongoing studies support the direct interaction of **YQ-II-128** with the NLRP3 protein (unpublished data). Although preliminary pharmacokinetic studies demonstrated **YQ-II-128** is a blood brain barrier penetrant, its permeability is limited and this compound also exhibits poor oral bioavailability, likely due to poor GI solubility and high first-pass effects. Herein, we report the structural modifications of **YQ-II-128** to understand how structural modifications on this chemical scaffold impact biological activity and to improve the aqueous solubility of these analogs by structure activity relationship (SAR) studies.

Molecular design and chemistry

To improve the aqueous solubility and explore whether further modifications of **YQ-II-128** will improve its inhibitory potency, a series of analogs were designed and synthesized. As shown in Fig. 3, structural modifications were mainly focused on three positions of **YQ-II-128** to incorporate amine or hydroxyl containing moieties. Previous SAR study suggested the important roles of the propoxyl substituent of the lead compound. Therefore, analogs **2** and **3** are designed to include a morpholine or OH at the terminal position of the propoxyl substituent. In analog **4**, the propargyl moiety was

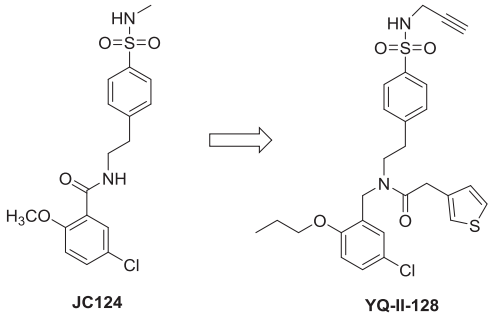

Fig. 2 Development of YQ-II-128 as a NLRP3 inhibitor

changed to a piperazine as our previous SAR studies suggested the tolerance of a tertiary sulfonamide at this position, and tertiary sulfonamide may increase the BBB penetration [27, 34]. Analogs **5–13** were designed to replace the thiophen-3-yl acetyl moiety with amino acids or acid with an amine moiety to improve aqueous solubility.

The chemical syntheses were achieved by the conditions shown in Scheme 1. Briefly, intermediate **14** was synthesized as we described previously [27]. Upon coupling with propargylamine or piperazine, reactions with hydrazine yielded **16** and **18**, respectively. Aldehydes **21**, **24**, and **26** were obtained by alkylation of chlorosalicylaldehyde **19**, which was followed by reductive amination with **16** and **18** to give **22**, **25**, **27**, or **28**, respectively. Finally, coupling reactions of **22**, **25**, **27,** or **28** with corresponding acids in the presence of EDCI and HOBt to yield target compounds **2–13**, respectively.

Results and discussion

After chemical synthesis, the target compounds were tested for their inhibitory potencies on the production of IL-1β in

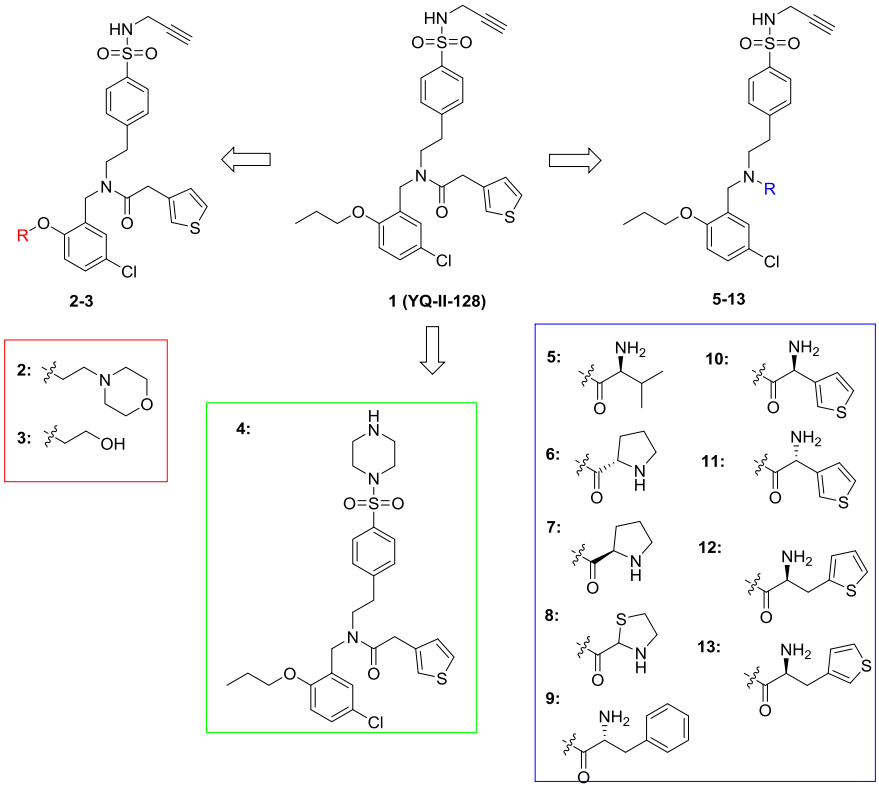

Fig. 3 Chemical structures of the designed analogs of YQ-II-128

mouse macrophage J774A.1 cells upon activation with LPS/ATP, a well-established assay for the NLRP3 inflammasome activity. As showed in Table 1, incorporation of a morpholine or an OH at the terminal position of the propoxyl substituent, as evidenced by **2** and **3**, led to a decreased inhibitory potency (nine- and sixfold, respectively) compared to that of **YQ-II-128**. This may hint that steric and hydrophobic interactions at this position are important for the biological activity. Replacement of the propargyl moiety in **YQ-II-128** with a piperazine moiety also led to a fourfold loss of potency under the current experimental settings. Our previous SAR studies of JC124 demonstrated a comparable potency by the same structural modification at this position. This may suggest that analogs based on the scaffolds of JC124 and **YQ-II-128** interact with the NLRP3 protein differently. But comparison of a full spectra of SAR studies are warranted to draw any conclusion. Surprisingly, the analogs with an amino acid moiety on the amide position (compounds **5–9**) all showed reduced inhibitory potency compared to that of **YQ-II-128** with analog **9** being the most potent in this series. The results may hint that an aromatic moiety is needed at this position to optimally interact with the NLRP3 protein. Adding an NH_2 moiety to the alpha-carbon of the thiophen-3-yl acetamide resulted an analog **10** with approximately twofold loss of potency. Interestingly, the *S*-isomer (**10**) is 2× more potent than the *R*-isomer (**11**), thus suggesting a role of stereochemistry on biological activity in this domain. Extension of one carbon on the amide domain as reflected by analogs **12** and **13** retained the inhibitory potency as that of **10**. The results of **12** and **13** also indicate that the substitution position on the thiophene ring is not critical for biological activity. The results of **10–13** also support the notion that the presence of an aromatic moiety is important for biological activity in the amide domain.

After the establishment of inhibitory potency on IL-1β release in J774A.1 cells, we selected **10** and **12**, the most potent analogs among this series, to evaluate their selectivity on the NLRP3 inflammasome. To this end, J774A.1 cells were stimulated with LPS/poly(dA:dT) or LPS/flagellin to activate the NLRC4 and AIM2 inflammasome, respectively. As shown in Fig. 4, compound **12** also significantly inhibited the NLRC4 and AIM2 inflammasomes at 10 μM while compound **10** did not show significant inhibition on these inflammasomes at this concentration. The results suggest that although no difference was observed on the inhibition of IL-1β production upon activation of the NLRP3 inflammasome by both compounds, structurally extended analog **12** lost the selective inhibition on NLRP3 inflammasome. This also suggests that steric interaction at this domain is limited with the NLRP3 protein. We also measured the solubility of **10** and **YQ-II-128** in water at pH of 7.4. As expected, analog **10** with a primary NH_2 moiety shows improved solubility of 19.5 ± 4.7 μg/ml, compared to **YQ-II-128** at 6.3 ± 1.1 μg/ml.

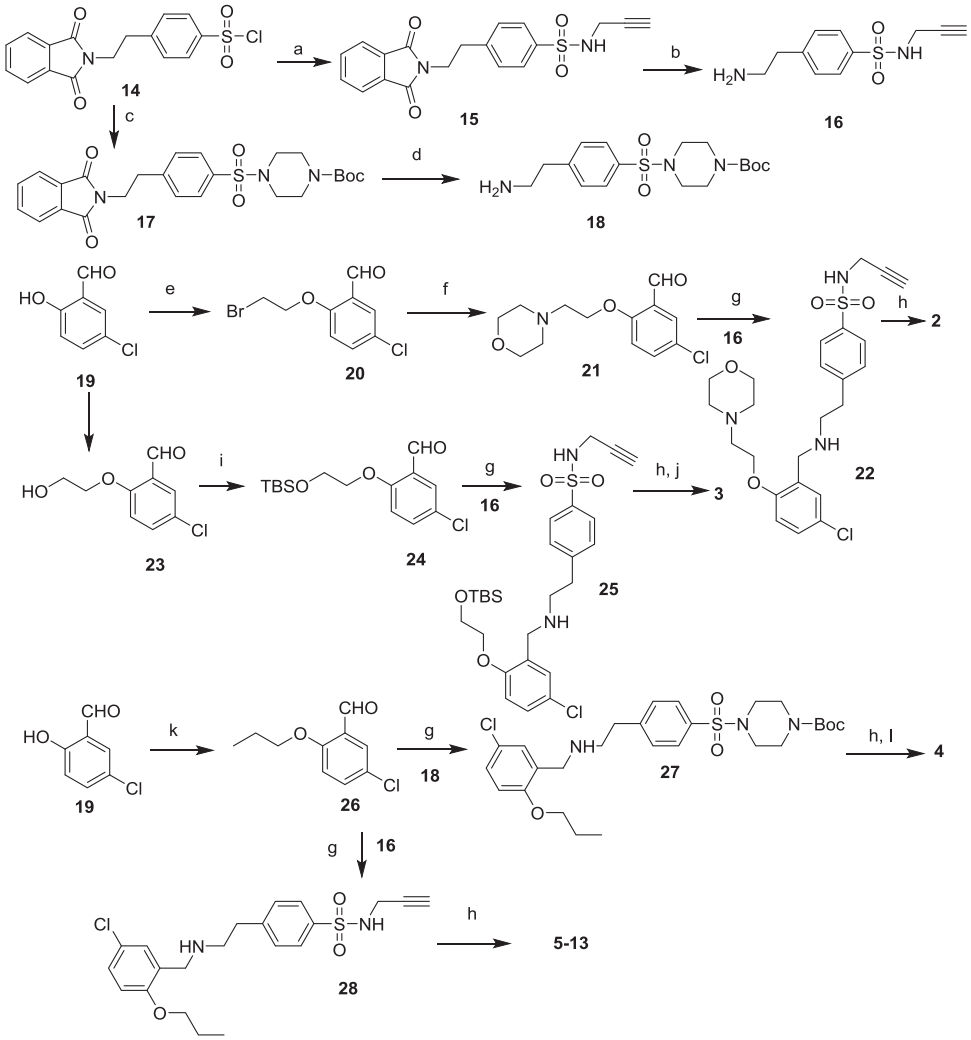

Scheme 1 Reactants and conditions: **a** propargylamine, TEA, DCM; **b d** NH_2NH_2, EtOH, 60 °C; **c** 1-(tert-Butoxycarbonyl) piperazine, TEA, DCM; **e** 1, 2-Dibromoethane, K_2CO_3, CH_3CN; **f** morphine, K_2CO_3, CH_3CN; **g** acetic acid, $NaCNBH_3$; **h** various acids, EDCI, HOBt, TEA, DCM; **i** TBSCl, imidazole, DCM; **j** 1M TBAF, THF; **k** 1-bromopropane, K_2CO_3, DMF; **l** TFA, DCM

Summary

In our efforts to develop small molecule inhibitors by targeting the NLRP3 inflammasome, we conducted SAR studies of a lead NLRP3 inhibitor, **YQ-II-128**, that was recently identified from our laboratory from a sulfonamide based chemical scaffold. The design of the new analogs was focused on incoporation of polar moieties, such as amine and OH, to improve aquesous solubility. The results revealed that steric interactions play important roles at the propoxyl and the amide domains of **YQ-II-128**. Furthermore, the presence of an aromatic moiety is necessary for optimla inhibitory potency at the amide domain. Among the series of analogs designed and charatcerized herein, analog **10** showed slightly reduced inhibitory potency while maintained selective inhibition on the NLRP3 inflammasome, and exhibited improved aqeous solubility. Collectively, the results strongly encourage further charactrization and development of analogs of **10** as NLRP3 inhibitors and exploring their therapeutic potentials for human diseases.

Experimental section

Materials and instrumentation

All chemicals and reagents used in the experiments were of analytical grade and obtained from Sigma-Aldrich. Operation process was monitored by thin layer chromatography (precoated silica gel 60 F254 plates, EMD Chemicals) and visualized with UV light or by treatment with phosphomolybdic acid. Flash chromatography was performed on silica gel (200–300 mesh, Fisher Scientific) using solvents as indicated. ^{1}H-NMR and ^{13}C-NMR spectra were routinely recorded on a Bruker ARX 400 spectrometer. The NMR solvent used was $CDCl_3$ or DMSO-d6 as indicated. Tetramethylsilane was used as internal standard.

Chemistry

4-(2-(1,3-Dioxoisoindolin-2-yl)ethyl)-N-(prop-2-yn-1-yl)-benzenesulfonamide (**15**).

Table 1 Inhibitory potency of the designed analogs on the production of IL-1β by J774A.1 cells upon stimulation with LPS/ATP

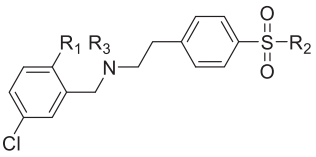

Compound	R_1	R_2	R_3	IC_{50} (μM)
2	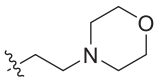	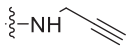	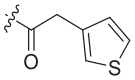	2.9 ± 0.9
3	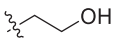	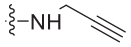	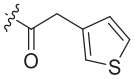	1.8 ± 0.1
4	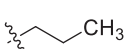	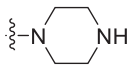	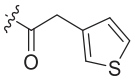	1.2 ± 0.2
5	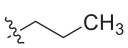	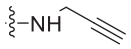	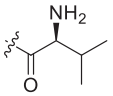	4.5 ± 0.9
6	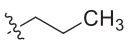	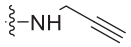	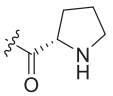	3.4 ± 0.2
7	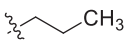	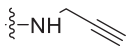	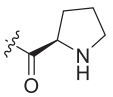	3.9 ± 1.5
8	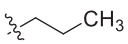	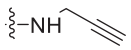	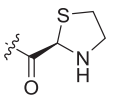	2.1 ± 0.5
9	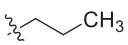	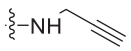	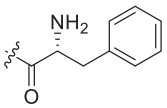	1.2 ± 0.1
10	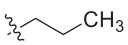	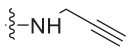	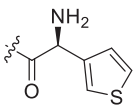	0.7 ± 0.1
11	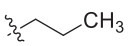	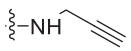	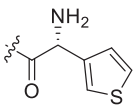	1.4 ± 0.4
12	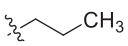	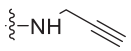	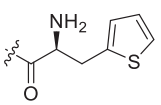	0.7 ± 0.2
13	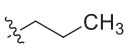	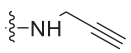	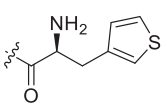	0.9 ± 0.1
YQ-II-128	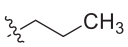	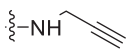	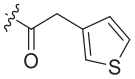	0.3 ± 0.01

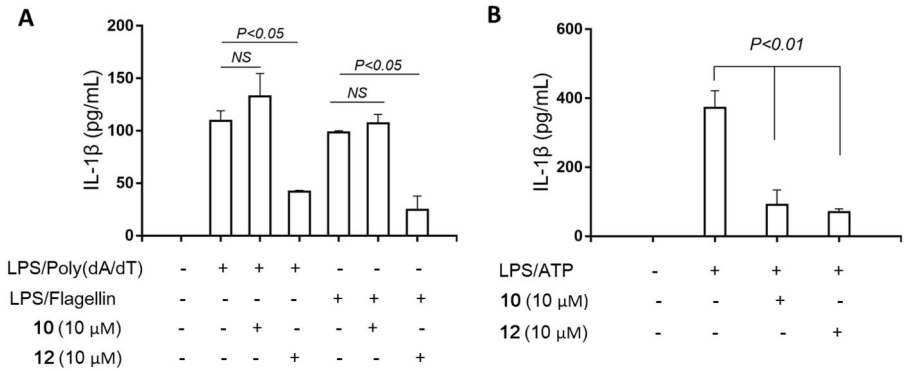

Fig. 4 **A**, **B** J774A.1 cells were primed with LPS (1 μg/ml) and activated with ATP (5 mM), flagellin (1 μg/ml), or poly(dA:dT) (4 μg/ml). Compounds were added when ATP, flagellin or poly(dA:dT) was added. Supernatants were then collected for IL-1β analysis by ELISA. Experiments were conducted in triplicate and repeated at least three time and Error bars represent SEM. Statistical analysis by Student *t* test

To the solution of **14** (3.0 g, 8.5 mmol) in acetonitrile (50 ml) were added propargylamine (1.1 ml, 17.0 mmol) and trimethylamine (2.4 ml, 17.0 mmol). The solution was stirred at room temperature (RT) for 4 h. The solvent was removed by vacuum. Dichloromethane (DCM) was added and the organic layer was washed with H_2O, dried over Na_2SO_4, concentrated, and purified by column chromatography (DCM/MeOH = 100/1) to give **15** (2.3 g, 75%) as a white solid. ^{1}H NMR (400 MHz $CDCl_3$): δ 3.04 (t, J = 7.44 Hz, 2H), 3.74–3.76 (m, 2H), 3.91 (t, J = 7.32 Hz, 2H), 4.67 (s, 1H), 7.31–7.39 (m, 2H), 7.63–7.77 (m, 6H).

4-(2-Aminoethyl)-N-(prop-2-yn-1-yl)benzenesulfonamide (**16**).

Hydrazine (0.8 ml, 25.0 mmol) was added dropwise to a solution of **15** (1.8 g, 5.0 mmol) in EtOH (30 ml). After addition, the solution was heated to 60 °C for 1 h. Then H_2O (100 ml) was added and extracted with DCM (3 × 20 ml). The organic layer was collected, dried over Na_2SO_4, and concentrated to give compound **15** as a yellow liquid without purification (0.94 g, 79%). ^{1}H NMR (400 MHz MeOD): δ 2.47 (d, J = 2.56 Hz, 1H), 2.84–2.95 (m, 4H), 3.76 (d, J = 2.52 Hz, 2H), 7.44 (d, J = 8.32 Hz, 2H), 7.83 (d, J = 8.36 Hz, 2H).

tert-butyl4-((4-(2-(1,3-dioxoisoindolin-2-yl)ethyl)phenyl)sulfonyl)piperazine-1-carboxylate (**17**)

Compound **17** was synthetized following the procedure of compound **15**.

^{1}H NMR (400 MHz, Chloroform-d) δ 7.91–7.82 (m, 1H), 7.74 (m, 2H), 7.65 (h, J = 3.7, 3.1 Hz, 2H), 7.59–7.49 (m, 1H), 7.40 (m, 1H), 7.34–7.29 (m, 1H), 3.93 (m, 2H), 3.43 (m, 4H), 3.36–2.97 (m, 4H), 2.84 (d, J = 5.9 Hz, 2H), 1.40–1.32 (m, 9H).

2-(2-bromoethoxy)-5-chlorobenzaldehyde (**20**)

Compound **19** (3 g, 19 mmol) and 1, 2-Dibromoethane (16.5 ml, 190 mmol) were dissolved in dry CH_3CN (50 ml), then K_2CO_3 (3.93 g, 28.5 mmol) was added and refluxed for 18 h. The reaction mixture was cooled to RT and filtered, washed with CH_3CN and evaporated to dry. The desired product was purified by column with hexane/acetate = 15:1 as eluent in 85% yield. ^{1}H NMR (400 MHz, Chloroform-d) δ 10.39 (d, J = 1.2 Hz, 1H), 7.92–7.63 (m, 1H), 7.42 (dt, J = 9.1, 1.9 Hz, 1H), 6.85 (d, J = 8.8 Hz, 1H), 4.56–4.19 (m, 2H), 3.86–3.50 (m, 2H).

5-chloro-2-(2-morpholinoethoxy)benzaldehyde (**21**)

Compound **20** (2.5 g, 9.5 mmol) and morphine (0.83 ml, 9.5 mmol) were dissolved in dry CH_3CN (30 ml), then K_2CO_3 (1.96 g, 14.22 mmol) was added and refluxed for overnight. The reaction mixture was cooled to RT and filtered, the organic layer was collected, evaporated and purified by column using acetate/methanol = 40:1 as eluent (yield: 78%).

^{1}H NMR (400 MHz, Chloroform-d) δ 10.33 (s, 1H), 7.72 (d, J = 2.7 Hz, 1H), 7.42 (dd, J = 8.9, 2.7 Hz, 1H), 6.89 (d, J = 8.9 Hz, 1H), 4.20 (s, 2H), 3.69 (s, 4H), 2.85 (s, 2H), 2.58 (s, 4H).

5-chloro-2-(2-hydroxyethoxy)benzaldehyde (**23**)

Compound **19** (1.56 g, 10 mmol) was added drop wise over 15 min to a vigorously stirred solution of sodium hydroxide (0.4 g, 10 mmol) in water (15 ml), and then 2-Bromoethanol (709 μL, 10 mmol) was added dropwise and the resulting solution was heated to reflux for 16 h. The solution was cooled and maintained at about 10 °C while sodium hydroxide was added until the solution was strongly alkaline (pH = 10). The reaction mixture was extracted with DCM (×4). The combined organic layers were dried and purified by column (hexane: acetate = 1:1) (yield: 71%).

^{1}H NMR (400 MHz, Chloroform-d) δ 10.33 (d, J = 13.5 Hz, 1H), 7.70 (dd, J = 6.0, 2.8 Hz, 1H), 7.41 (dd, J = 8.9, 2.8 Hz, 1H), 6.99–6.82 (m, 1H), 4.12 (q, J = 8.6, 6.4 Hz, 2H), 3.96 (p, J = 5.2, 4.7 Hz, 2H).

2-(2-((tert-butyldimethylsilyl)oxy)ethoxy)-5-chlorobenzaldehyde (**24**)

TBSCl (0.68 g, 4.56 mmol) was added to the solution of compound **23** (0.45 g, 2.28 mmol) and imidazole (0.23 g,

3.42 mmol) in DCM (10 ml). The mixture was stirred at RT overnight. After reaction completion, the DCM was washed with DI water and brine, evaporated and purified by column (hexane/acetate = 20:1) to yield the product as a white solid in 89% yield.

^{1}H NMR (400 MHz, Chloroform-d) δ 10.51–10.12 (m, 1H), 7.70 (dd, J = 2.9, 1.4 Hz, 1H), 7.40 (ddd, J = 11.4, 9.2, 2.7 Hz, 1H), 6.90 (dd, J = 9.0, 4.4 Hz, 1H), 4.11 (dt, J = 17.5, 4.8 Hz, 2H), 3.94 (dt, J = 14.1, 4.8 Hz, 2H), 0.91–0.72 (m, 9H), 0.04–0.01 (m, 6H).

5-chloro-2-propoxybenzaldehyde (**26**)

A mixture of compound **19** (1.6 g, 10 mmol), 1-bromopropane (1.3 g, 11.0 mmol) and and K_2CO_3 (2.75 g, 20 mmol) in DMF (30 ml) was stirred at RT for 48 h. DMF was evaporated under reduced pressure, and the residue was taken up to DCM (30 ml). The DCM solution was washed with water thrice, dried over anhydrous Na2SO4, filtered, and evaporated to obtain product as a yellow solid and was used in the next step without any further purification (yield: 85%).

^{1}H NMR (400 MHz DMSO-d6): δ 1.03 (t, J = 7.40 Hz, 3H), 1.75–1.84 (m, 2H), 4.12 (t, J = 6.40 Hz, 2H), 7.29 (d, J = 8.92 Hz, 1H), 7.62 (d, J = 2.80 Hz, 1H), 7.69 (dd, $J1$ = 2.84 Hz, $J2$ = 8.96 Hz, 1H), 10.33 (s, 1H).

4-(2-((5-chloro-2-propoxybenzyl)amino)ethyl)-N-(prop-2-yn-1-yl)benzenesulfonamide (**28**)

Compound **26** (2.0 g, 10 mmol) and compound **16** (2.4 g, 10 mmol) were dissolved in 1, 2-dichloroethane (30 ml) and stirred at RT for 1 h. Then, acetic acid (343 µL, 6 mmol) was added, and the mixture was stirred at RT for another 1 h. $NaCNBH_3$ (0.67 g, 10 mmol) in methanol was added portion wise. Then, the reaction was stirred at RT for 4 h. The reactant was washed with water, brine, dried over anhydrous Na_2SO_4, and evaporated under vacuum. The crude product was purified by chromatography using hexane/acetate = 1/1 to get target compound as oil in 57% yield.

^{1}H NMR (400 MHz DMSO-d6): δ 0.97 (t, J = 7.68 Hz, 3H), 1.64–1.73 (m, 2H), 2.81-2.84 (m, 4H), 3.05 (t, J = 2.52 Hz, 1H), 3.65–3.66 (m, 2H), 3.72 (s, 2H), 3.92 (t, J = 6.36 Hz, 2H), 6.97 (d, J = 8.72 Hz, 1H), 7.25 (dd, $J1$ = 2.76 Hz, $J2$ = 8.68 Hz, 1H), 7.33 (d, J = 2.72 Hz, 1H), 7.43 (d, J = 8.36 Hz, 2H), 7.72 (d, J = 8.36 Hz, 2H), 8.05 (s, 1H).

Compounds **22**, **25** and **27** were synthesized following the procedure of compound **28**.

N-(5-chloro-2-(2-morpholinoethoxy)benzyl)-N-(4-(N-(prop-2-yn-1-yl)sulfamoyl)phenethyl)-2-(thiophen-3-yl) acetamide (**2**)

3-Thiopheneacetic acid (0.3 g, 2.1 mmol), EDCI (0.4 g, 2.1 mmol) and HOBt (0.28 g, 2.1 mmol) were dissolved in anhydrous dichloromethane (10 ml) under an ice bath followed by the addition of TEA (292 µL, 2.1 mmol). The mixture was stirred at RT for 30 min. Compound **22** (0.49 g, 1.0 mmol) was added and the reaction was stirred at RT for 3 h. The reactant was then washed with saturated $NaHCO_3$, and brine. DCM layer was collected and concentrated and purified by column chromatography (DCM/MeOH = 30/1) to give desired compound as a white solid in 69% yield.

^{1}H NMR (400 MHz, DMSO-d6) δ 8.00 (dt, J = 13.8, 5.9 Hz, 1H), 7.63 (ddd, J = 24.4, 9.6, 3.1 Hz, 2H), 7.44–7.32 (m, 2H), 7.28–7.08 (m, 3H), 7.05–6.78 (m, 3H), 4.38 (d, J = 6.6 Hz, 2H), 4.05 (dd, J = 10.4, 5.2 Hz, 2H), 3.70–3.27 (m, 9H), 3.00–2.48 (m, 5H), 2.37 (d, J = 9.3 Hz, 4H). ^{13}C NMR (101 MHz, DMSO) δ 170.72, 144.60, 139.01, 136.00, 130.04, 129.69, 129.15, 128.97, 128.53, 128.17, 127.32, 127.25, 126.38, 122.72, 114.07, 79.82, 75.05, 66.61, 53.93, 47.00, 43.59, 35.36, 34.80, 34.61, 33.32, 32.37. HRMS (AP-ESI) *m/z*: calcd for $C_{30}H_{34}ClN_3O_5S_2$ $[M+H]^+$ 616.1707; found, 616.1711.

Compounds **3**–-**13** were synthesized following the procedure of compound **2**.

N-(5-chloro-2-(2-hydroxyethoxy)benzyl)-N-(4-(N-(prop-2-yn-1-yl)sulfamoyl)phenethyl)-2-(thiophen-3-yl)acetamide (**3**)

^{1}H NMR (400 MHz, DMSO-d6) δ 8.06 (dt, J = 12.2, 5.9 Hz, 1H), 7.76-7.64 (m, 2H), 7.51–7.41 (m, 2H), 7.38–7.12 (m, 3H), 7.08–6.91 (m, 3H), 4.88 (q, J = 6.0 Hz, 1H), 4.53 (d, J = 3.2 Hz, 2H), 4.05 (dt, J = 13.4, 4.9 Hz, 2H), 3.78–3.41 (m, 7H), 3.02 (dt, J = 3.6, 2.4 Hz, 1H), 2.83 (dt, J = 33.0, 7.6 Hz, 2H). ^{13}C NMR (101 MHz, DMSO) δ 170.80, 155.73, 144.01, 138.97, 136.00, 130.06, 129.69, 129.14, 128.67, 128.04, 127.31, 126.39, 124.57, 122.83, 114.05, 79.82, 75.05, 70.83, 60.04, 49.31, 46.83, 35.19, 33.28, 32.37. HRMS (AP-ESI) *m/z*: calcd for $C_{26}H_{27}ClN_2O_5S_2$ $[M+Na]^+$ 569.0947; found, 569.0948.

N-(5-chloro-2-propoxybenzyl)-N-(4-(piperazin-1-ylsulfonyl)phenethyl)-2-(thiophen-3-yl)acetamide (**4**)

^{1}H NMR (400 MHz, DMSO-d6) δ 7.80–7.49 (m, 4H), 7.50–7.18 (m, 3H), 7.13–6.92 (m, 3H), 4.50 (d, J = 9.3 Hz, 2H), 4.24–3.50 (m, 8H), 3.03–2.70 (m, 9H), 1.77 (dt, J = 13.2, 6.7 Hz, 2H), 1.01 (q, J = 7.6 Hz, 3H). ^{13}C NMR (101 MHz, DMSO) δ 170.74, 155.60, 144.80, 135.98, 133.41, 130.31, 129.11, 128.98, 128.23, 128.14, 127.92, 126.42, 124.42, 122.83, 113.69, 70.04, 49.35, 46.77, 44.88, 43.55, 35.28, 34.81, 22.47, 10.94. HRMS (AP-ESI) *m/z*: calcd for $C_{28}H_{34}ClN_3O_4S_2$ $[M+H]^+$ 576.1758; found, 576.1755.

(S)-2-amino-N-(5-chloro-2-propoxybenzyl)-3-methyl-N-(4-(N-(prop-2-yn-1-yl)sulfamoyl)phenethyl)butanamide (**5**)

^{1}H NMR (400 MHz, DMSO-d6) δ 8.28-8.06 (m, 3H), 7.80–7.66 (m, 2H), 7.51 (d, J = 8.2 Hz, 1H), 7.25 (m, 1H), 7.14–6.99 (m, 1H), 4.72–3.81 (m, 5H), 3.82-3.45 (m, 2H), 3.31–2.53 (m, 3H), 2.24–1.87 (m, 1H), 1.73 (m, 2H), 1.04–0.67 (m, 9H). ^{13}C NMR (101 MHz, DMSO) δ 169.19, 155.65, 144.10, 138.92, 131.26, 129.95, 128.54, 127.51,

127.32, 124.75, 114.17, 79.82, 75.07, 70.27, 54.85, 49.15, 34.86, 32.36, 30.29, 22.33, 19.21, 16.84, 10.86. HRMS (AP-ESI) *m/z*: calcd for $C_{26}H_{34}ClN_3O_4S$ $[M+H]^+$ 520.2037; found, 520.2040.

(S)-N-(5-chloro-2-propoxybenzyl)-N-(4-(N-(prop-2-yn-1-yl)sulfamoyl)phenethyl)pyrrolidine-2-carboxamide (**6**)

^{1}H NMR (400 MHz, DMSO-d6) δ 8.01 (s, 1H), 7.64 (M, 2H), 7.40 (d, J = 7.8 Hz, 1H), 7.34–6.85 (m, 4H), 4.55–4.15 (m, 2H), 3.88 (m, 2H), 3.56 (d, J = 18.7 Hz, 2H), 3.10–2.67 (m, 6H), 1.83–1.46 (m, 4H), 1.05 (t, J = 7.2 Hz, 4H), 0.89 (dt, J = 10.6, 7.3 Hz, 3H). ^{13}C NMR (101 MHz, DMSO) δ 172.38, 155.82, 143.64, 139.31, 129.97, 129.80, 128.50, 128.43, 127.32, 124.40, 114.04, 79.81, 75.08, 70.12, 58.27, 58.04, 46.57, 46.08, 32.35, 29.92, 29.76, 22.31, 10.82, 9.83. HRMS (AP-ESI) *m/z*: calcd for $C_{26}H_{32}ClN_3O_4S$ $[M+H]^+$ 518.1880; found, 518.1875.

(R)-N-(5-chloro-2-propoxybenzyl)-N-(4-(N-(prop-2-yn-1-yl)sulfamoyl)phenethyl)pyrrolidine-2-carboxamide (**7**)

^{1}H NMR (400 MHz, DMSO-d6) δ 8.10 (q, J = 5.9 Hz, 1H), 7.79–7.60 (m, 2H), 7.56–7.42 (m, 1H), 7.42–6.93 (m, 4H), 4.69–4.39 (m, 2H), 4.03-3.93 (m, 2H), 3.72-3.58 (m, 2H), 3.28-2.57 (m, 6H), 2.08-1.51 (m, 4H), 1.46-1.16 (m, 4H), 0.96 (M, 3H). ^{13}C NMR (101 MHz, DMSO) δ 169.01, 158.62, 144.07, 139.14, 129.97, 128.76, 127.32, 127.27, 126.27, 119.50, 113.91, 78.89, 75.07, 70.14, 58.34, 58.18, 47.25, 46.06, 32.36, 29.57, 24.00, 22.29, 10.93, 9.02. HRMS (AP-ESI) *m/z*: calcd for $C_{26}H_{32}ClN_3O_4S$ $[M+H]^+$ 518.1880; found, 518.1875.

(R)-N-(5-chloro-2-propoxybenzyl)-N-(4-(N-(prop-2-yn-1-yl)sulfamoyl)phenethyl)thiazolidine-2-carboxamide (**8**)

^{1}H NMR (400 MHz, DMSO-d6) δ 8.01 (m, 1H), 7.76-7.54 (m, 2H), 7.49-7.06 (m, 3H), 7.06–6.77 (m, 2H), 4.60–4.20 (m, 2H), 4.03–3.77 (m, 2H), 3.64-3.55 (m, 2H), 3.15–2.50 (m, 6H), 1.65 (m, 2H), 1.30-0.78 (m, 6H). ^{13}C NMR (101 MHz, DMSO) δ 177.13, 155.82, 138.98, 138.69, 130.06, 130.03, 129.77, 128.33, 127.28, 124.55, 113.80, 79.82, 75.07, 70.09, 61.20, 56.79, 48.73, 32.37, 29.49, 29.15, 22.48, 10.95, 10.92. HRMS (AP-ESI) *m/z*: calcd for $C_{25}H_{30}ClN_3O_4S_2$ $[M+Na]^+$ 558.1264; found, 558.1260.

(R)-2-amino-N-(5-chloro-2-propoxybenzyl)-3-phenyl-N-(4-(N-(prop-2-yn-1-yl)sulfamoyl)phenethyl)propanamide (**9**)

^{1}H NMR (400 MHz, DMSO-d6) δ 7.76 (dd, J = 8.3, 3.1 Hz, 2H), 7.29 (m, 8H), 7.10–6.93 (m, 2H), 4.42–4.27 (m, 2H), 3.98 (q, J = 6.0 Hz, 2H), 3.77–3.45 (m, 3H), 3.08 (m, 1H), 2.94–2.62 (m, 4H), 2.09–1.62 (m, 4H), 1.01 (m, 3H). ^{13}C NMR (101 MHz, DMSO) δ 175.39, 155.53, 143.96, 138.92, 129.79, 129.73, 129.63, 128.57, 128.31, 128.09, 127.29, 126.63, 124.65, 124.40, 113.77, 79.82, 75.01, 70.00, 53.13, 48.62, 43.69, 42.75, 35.07, 32.36, 22.46, 10.95. HRMS (AP-ESI) *m/z*: calcd for $C_{30}H_{34}ClN_3O_4S$ $[M+H]^+$ 568.2037; found, 568.2039.

(S)-2-amino-N-(5-chloro-2-propoxybenzyl)-N-(4-(N-(prop-2-yn-1-yl)sulfamoyl)phenethyl)-2-(thiophen-3-yl) acetamide (**10**)

^{1}H NMR (400 MHz, DMSO-d6) δ 7.99 (s, 1H), 7.70–7.39 (m, 3H), 7.38-7.08 (m, 3H), 7.08-6.67 (m, 3H), 5.08 (d, J = 72.0 Hz, 1H), 4.57–4.03 (m, 2H), 3.85 (m, 2H), 3.52 (d, J = 43.1 Hz, 3H), 2.95 (s, 1H), 2.86–2.56 (m, 1H), 1.61 (m, 2H), 0.87 (m, 3H). ^{13}C NMR (101 MHz, DMSO) δ 171.79, 155.48, 143.63, 139.00, 129.90, 129.73, 128.73, 128.16, 127.77, 127.48, 127.30, 127.25, 127.12, 124.40, 113.67, 79.80, 75.03, 70.06, 50.93, 48.77, 44.26, 34.53, 32.37, 22.43, 10.92. HRMS (AP-ESI) *m/z*: calcd for $C_{27}H_{30}ClN_3O_4S_2$ $[M+H]^+$ 560.1425; found, 560.1427.

(R)-2-amino-N-(5-chloro-2-propoxybenzyl)-N-(4-(N-(prop-2-yn-1-yl)sulfamoyl)phenethyl)-2-(thiophen-3-yl) acetamide (**11**)

^{1}H NMR (400 MHz, DMSO-d6) δ 8.07 (s, 1H), 7.79–7.46 (m, 3H), 7.46–7.18 (m, 3H), 7.17–6.93 (m, 2H), 6.86 (d, J = 10.6 Hz, 1H), 5.33–4.87 (m, 1H), 4.67-4.08 (m, 2H), 3.94 (m, 2H), 3.60 (d, J = 43.7 Hz, 3H), 3.03 (s, 1H), 2.94–2.66 (m, 1H), 1.69 (m, 2H), 0.94 (m, 3H). ^{13}C NMR (101 MHz, DMSO) δ 171.77, 155.50, 143.65, 139.02, 129.90, 129.74, 128.74, 128.18, 127.93, 127.50, 127.32, 127.26, 127.13, 124.42, 113.70, 79.82, 75.04, 70.07, 51.10, 48.78, 44.25, 34.53, 32.37, 22.44, 10.92. HRMS (AP-ESI) *m/z*: calcd for $C_{27}H_{30}ClN_3O_4S_2$ $[M+H]^+$ 560.1445; found, 560.1446.

(S)-2-amino-N-(5-chloro-2-propoxybenzyl)-N-(4-(N-(prop-2-yn-1-yl)sulfamoyl)phenethyl)-3-(thiophen-2-yl) propanamide (**12**)

^{1}H NMR (400 MHz, DMSO-d6) δ 8.11 (s, 1H), 7.76 (d, J = 7.8 Hz, 2H), 7.45–7.22 (m, 4H), 7.09–6.93 (m, 3H), 6.86 (d, J = 21.7 Hz, 1H), 4.45 (d, J = 35.0 Hz, 2H), 3.94 (m, 3H), 3.82–3.50 (m, 4H), 3.21–3.02 (m, 2H), 3.01–2.65 (m, 3H), 1.77 (m, 2H), 1.01 (m, 3H). ^{13}C NMR (101 MHz, DMSO) δ 174.92, 155.52, 143.93, 138.96, 129.82, 129.75, 128.27, 128.07, 127.96, 127.32, 127.11, 126.48, 124.80, 124.47, 113.60, 79.83, 75.00, 70.03, 55.36, 53.29, 48.83, 43.84, 36.51, 32.36, 22.47, 10.94. HRMS (AP-ESI) *m/z*: calcd for $C_{28}H_{32}ClN_3O_4S_2$ $[M+H]^+$ 596.1420; found, 596.1417.

(S)-2-amino-N-(5-chloro-2-propoxybenzyl)-N-(4-(N-(prop-2-yn-1-yl)sulfamoyl)phenethyl)-3-(thiophen-3-yl) propanamide (**13**)

^{1}H NMR (400 MHz, DMSO-d6) δ 8.13 (d, J = 15.2 Hz, 1H), 7.76 (dd, J = 8.3, 3.2 Hz, 2H), 7.52-7.22 (m, 4H), 7.18 (dd, J = 8.9, 2.4 Hz, 1H), 7.12–6.85 (m, 3H), 4.40 (d, J = 4.2 Hz, 2H), 3.99 (t, J = 6.4 Hz, 2H), 3.86 (t, J = 6.9 Hz, 1H), 3.75–3.45 (m, 4H), 3.15–3.01 (m, 1H), 2.99–2.63 (m, 4H), 1.85–1.65 (m, 2H), 1.01 (m, 3H). ^{13}C NMR (101 MHz, DMSO) δ 175.39, 155.52, 143.99, 139.27, 129.87, 129.74, 129.48, 128.33, 128.09, 127.29, 127.27, 126.10, 124.43, 122.50, 113.61, 79.82, 75.03, 70.01, 52.55, 52.36,

48.69, 43.74, 36.91, 32.35, 22.47, 10.91. HRMS (AP-ESI) *m/z*: calcd for $C_{28}H_{32}ClN_3O_4S_2$ $[M+H]^+$ 596.1420; found, 596.1421.

Biological assays

Cells

J774A.1 murine macrophage cells and was purchased from American Type Cell Culture (ATCC, Manassas, VA). J774A.1 cells were cultured in Dulbecco's modified Eagle medium (DMEM) with 10% fetal bovine serum (FBS), 1% penicillin/streptomycin. J774A.1 cells were used under passage 50 for the experiments. For cell-based assays, at least three independent experiments with at least triplicates for each data point of each experiment were conducted.

IL-1β assays in J774A.1 cells

J774A.1 cells were plated into 96-well plates (1×10^5 cells/well) for 16 h in growth medium. Cells were primed with Escherichia coli 0111:B4 LPS (Sigma-Aldrich) (final concentration: 1 μg/ml) for 4.5 h. Next, test compounds (0.1, 0.3, 1.0, 3.0, and 10.0 μM) were added and incubated for 30 min, followed by adding ATP (5 mM). After 30 min, the supernatants were collected, and the level of IL-1β was measured with a mouse IL-1β ELISA kit (DuoSet ELISA, R&D Systems) following the manufacturer's instructions.

Inhibition on the NLRC4 and AIM2 inflammasome assays

J774A.1 cells were plated into 96-well plates (1×10^5 cells/well) for 16 h in growth medium. Cells were treated with LPS (1 μg/ml) and test compounds for 1 h (10 μM). Flagellin or poly-deoxyadenylic−deoxythymidylic acid sodium salt (poly(dA:dT)) was used to induce the formation of the NLRC4 and the AIM2 inflammasomes. Flagellin (Enzo Life Sciences, Farmingdale, NY), isolated from Salmonella typhimurium strain 14028, was added in DMEM (Invitrogen) without FBS to the plate (1 μg/ml) and allowed to incubate for 6 h. Flagellin cell-transfection was accomplished utilizing the Polyplus transfection kit (PULSin, New York, NY). For AIM2 activation, cells were incubated with poly(dA:dT) (4 μg/ml) (InvivoGen, San Diego, CA) for 8 h. The supernatants were collected, and levels of IL-1β were measured with a mouse IL-1β ELISA kit following manufacturer's instructions.

Solubility test

Compounds were dissolved in DI water at 1 mg/ml, sonicated for 20 min, and then incubated at room temperature for 24 h. Samples were microfuged 2 times at 12,000 × *g* for 20 min each. Supernatants were analyzed using a Varian ProStar HPLC equipped with a Variable Wavelength UV–Visible Detector at 230 nm and Microsorb-MV C18 column 250 × 4.6 mm, isocratic solvent system A/B 60/40 or 75/25 in 12 min (**10** and YQ-II-128, respectively), A consisting of 0.1% TFA acetonitrile, B consisting of 0.1% TFA water, flow rate of 1 ml/min at room temperature. Standard curves were constructed by dissolving compounds in methanol or acetonitrile (**10** and YQ-II-128, respectively) and making serial dilutions.

Data accessibility

The datasets supporting this article have been included and could be found in the manuscript.

Acknowledgements The work was supported in part by the NIA of the NIH under award number R01AG058673 (SZ), Alzheimer's Drug Discovery Foundation 20150601 (SZ).

Author contributions YX and MS performed organic synthesis and biological characterization. HB tested the solubility. SZ designed the research. SZ and YX wrote the manuscript.

Compliance with ethical standards

Conflict of interest The authors declare that they have no conflict of interest.

References

1. Martinon F, Burns K, Tschopp J. The inflammasome: a molecular platform triggering activation of inflammatory caspases and processing of proIL-beta. Mol Cell. 2002;10:417–26. https://doi.org/10.1016/S1097-2765(02)00599-3
2. Schroder K, Tschopp J. The inflammasomes. Cell. 2010;140:821–32. https://doi.org/10.1016/j.cell.2010.01.040
3. Malik A, Kanneganti T-D. Inflammasome activation and assembly at a glance. J Cell Sci. 2017;130:3955–63. https://doi.org/10.1242/jcs.207365
4. Latz E, Xiao TS, Stutz A. Activation and regulation of the inflammasomes. Nat Rev Immunol. 2013;13:397–411. https://doi.org/10.1038/nri3452
5. Shao B-Z, Xu Z-Q, Han B-Z, Su D-F, Liu C. Nlrp3 inflammasome and its inhibitors: a review. Front Pharmacol. 2015;6:262. https://doi.org/10.3389/fphar.2015.00262
6. Kelly N, Jeltema D, Duan Y, He Y. The NLRP3 inflammasome: an overview of mechanisms of activation and regulation. Int J Mol Sci. 2019;20:3328. https://doi.org/10.3390/ijms20133328
7. Rowczenio DM, Gomes SM, Aróstegui JI, Mensa-Vilaro A, Omoyinmi E, Trojer H, et al. Late-onset cryopyrin-associated periodic syndromes caused by somatic NLRP3 mosaicism-UK single center experience. Front Immunol. 2017;8:1410. https://doi.org/10.3389/fimmu.2017.01410
8. Hoffman HM, Mueller JL, Broide DH, Wanderer AA, Kolodner RD. Mutation of a new gene encoding a putative pyrin-like

protein causes familial cold autoinflammatory syndrome and Muckle-Wells syndrome. Nat Genet. 2001;29:301–5. https://doi.org/10.1038/ng756
9. De Nardo D, Latz E. NLRP3 inflammasomes link inflammation and metabolic disease. Trends Immunol. 2011;32:373–9. https://doi.org/10.1016/j.it.2011.05.004
10. Choi AJS, Ryter SW. Inflammasomes: molecular regulation and implications for metabolic and cognitive diseases. Mol Cells. 2014;37:441–8. https://doi.org/10.14348/molcells.2014.0104
11. Couturier J, Stancu IC, Schakman O, Pierrot N, Huaux F, Kienlen-Campard P, et al. Activation of phagocytic activity in astrocytes by reduced expression of the inflammasome component ASC and its implication in a mouse model of Alzheimer's disease. J Neuroinflammation. 2016;13:20. https://doi.org/10.1186/s12974-016-0477-y
12. Freeman LC, Ting JP-Y. The pathogenic role of the inflammasome in neurodegenerative diseases. J Neurochem. 2016;136:29–38. https://doi.org/10.1111/jnc.13217
13. Heneka MT, Kummer MP, Stutz A, Delekate A, Schwartz S, Vieira-Saecker A, et al. Nlrp3 is activated in Alzheimer's disease and contributs to pathology in App/Ps1 Mice. Nature. 2013;493:674–8. https://doi.org/10.1038/nature11729
14. Venegas C, Kumar S, Franklin BS, Dierkes T, Brinkschulte R, Tejera D, et al. Microglia-derived ASC specks cross-seed amyloid-β in Alzheimer's disease. Nature. 2017;552:355–61. https://doi.org/10.1038/nature25158
15. Lazaridis L-D, Pistiki A, Giamarellos-Bourboulis EJ, Georgitsi M, Damoraki G, Polymeros D, et al. Activation of NLRP3 inflammasome in inflammatory bowel disease: differences between Crohn's disease and ulcerative colitis. Dig Dis Sci. 2017;62:2348–56. https://doi.org/10.1007/s10620-017-4609-8
16. Feist E, Burmester GR. Canakinumab for treatment of cryopyrin-associated periodic syndrome. Expert Opin Biol Ther. 2010;10:1631–6. https://doi.org/10.1517/14712598.2010.530653
17. Kelly A, Ramanan AV. A case of macrophage activation syndrome successfully treated with anakinra. Nat Clin Pract Rheumatol. 2008;4:615–20. https://doi.org/10.1038/ncprheum0919
18. Gillespie J, Mathews R, McDermott MF. Rilonacept in the management of cryopyrin-associated periodic syndromes (CAPS). J Inflamm Res. 2010;3:1–8. https://doi.org/10.2147/JIR.S8109
19. Zhang X, Xu A, Lv J, Zhang Q, Ran Y, Wei C, et al. Development of small molecule inhibitors targeting NLRP3 inflammasome pathway for inflammatory diseases. Eur J Med Chem. 2020;185:111822. https://doi.org/10.1016/j.ejmech.2019.111822
20. Coll RC, Robertson AAB, Chae JJ, Higgins SC, Muñoz-Planillo R, Inserra MC, et al. A small-molecule inhibitor of the NLRP3 inflammasome for the treatment of inflammatory diseases. Nat Med. 2015;21:248–55. https://doi.org/10.1038/nm.3806
21. Jiang H, Hongbin H, Chen Y, Huang W, Cheng J, Ye J, et al. Identification of selective and direct NLRP3 inhibitor to treat inflammatory disorders. J Exp Med. 2017;214:3219–38. https://doi.org/10.1084/jem.20171419
22. Wang S, Yang H, Yu L, Jin J, Qian L, Zhao H, et al. Oridonin attenuates $A\beta_{1-42}$-indicued neuroinflammation and inhibits NF-κB pathway. PLoS ONE. 2014;9:e104745. https://doi.org/10.1371/journal.pone.0104745
23. Huang Y, Jiang H, Chen Y, Wang X, Yang Y, Tao J, et al. Tranilast directly targets NLRP3 to treat inflammasome-driven diseases. EMBO Mol Med. 2018;10:e8689. https://doi.org/10.15252/emmm.201708689
24. He Y, Varadarajan S, Muñoz-Planillo R, Burberry A, Nakamura Y, Núñez G. 3,4-Methylenedioxy-β-nitrostyrene inhibits NLRP3 inflammasome activation by blocking assembly of the inflammasome. J Biol Chem. 2014;289:1142–50. https://doi.org/10.1074/jbc.M113.515080
25. Marchetti C, Swartzwelter B, Gamboni F, Neff CP, Richter K, Azam T, et al. OLT1177, a β-sulfonyl nitrile compound, safe in humans, inhibits the NLRP3 inflammasome and reverses the metabolic cost of inflammation. Proc Natl Acad Sci. 2018;115:E1530–39. https://doi.org/10.1073/pnas.1716095115
26. Cocco M, Pellegrini C, Martínez-Banaclocha H, Giorgis M, Marini E, Costale A, et al. Development of an acrylate derivative targeting the NLRP3 inflammasome for the treatment of inflammatory bowel disease. J Med Chem. 2017;60:3656–71. https://doi.org/10.1021/acs.jmedchem.6b01624
27. Fulp J, He L, Toldo S, Jiang Y, Boice A, Guo C, et al. Structural insights of benzenesulfonamide analogues as NLRP3 inflammasome inhibitors: design, synthesis, and biological characterization. J Med Chem. 2018;61:5412–23. https://doi.org/10.1021/acs.jmedchem.8b00733
28. Perera AP, Fernando R, Shinde T, Gundamaraju R, Southam B, Sohal SS, et al. MCC950, a specific small molecule inhibitor of NLRP3 inflammasome attenuates colonic inflammation in spontaneous colitis mice. Sci Rep. 2018;8:8618. https://doi.org/10.1038/s41598-018-26775-w
29. Xia S, Zhang X, Li C, Guan H. Oridonin inhibits breast cancer growth and metastasis through blocking the Notch signaling. Saudi Pharm J. 2017;25:638–43. https://doi.org/10.1016/j.jsps.2017.04.037
30. Sato S, Takahashi S, Asamoto M, Naiki T, Naiki-Ito A, Asai K, et al. Tranilast suppresses prostate cancer growth and osteoclast differentiation in vivo and in vitro. Prostate. 2009;70:229–38. https://doi.org/10.1002/pros.21056
31. Marchetti C, Swartzwelter B, Koenders MI, Azam T, Tengesdal IW, Powers N, et al. NLRP3 inflammasome inhibitor OLT1177 suppresses joint inflammation in murine models of acute arthritis. Arthritis Res Ther. 2018;20:169. https://doi.org/10.1186/s13075-018-1664-2
32. Yin J, Zhao F, Chojnacki J, Fulp J, Klein WL, Zhang S, et al. NLRP3 inflammasome inhibitor ameliorates amyloid pathology in a mouse model of Alzheimer's disease. Mol Neurobiol. 2018;55:1977–87. https://doi.org/10.1007/s12035-017-0467-9
33. Jiang Y, He L, Green J, Blevins H, Guo C, Harsiddhbhai S, et al. Discovery of second-generation NLRP3 inflammasome inhibitors: design, synthesis, and biological characterization. J Med Chem. 2019;62:9718–31. https://doi.org/10.1021/acs.jmedchem.9b01155
34. Brand S, Norcross NR, Thompson S, Harrison JR, Smith VC, Robinson DA, et al. Lead optimization of a pyrazole sulfonamide series of *Trypanosoma brucei N*-myristoyltransferase inhibitors: identification and evaluation of CNS penetrant compounds as potential treatments for stage 2 human African trypanosomiasis. J Med Chem. 2014;57:9855–69. https://doi.org/10.1021/jm500809c